Hindawi Publishing Corporation
Mathematical Problems in Engineering
Volume 2011, Article ID 451047, 15 pages
doi:10.1155/2011/451047

Research Article

Dynamics of an Autoparametric Pendulum-Like System with a Nonlinear Semiactive Suspension

Krzysztof Kecik and Jerzy Warminski

Department of Applied Mechanics, Lublin University of Technology, Nadbystrzycka 36, 20-618 Lublin, Poland

Correspondence should be addressed to Krzysztof Kecik, k.kecik@pollub.pl

Received 5 August 2010; Revised 30 November 2010; Accepted 27 December 2010

Academic Editor: Maria do Rosário de Pinho

This paper presents vibration analysis of an autoparametric pendulum-like mechanism subjected to harmonic excitation. To improve dynamics and control motions, a new suspension composed of a semiactive magnetorheological damper and a nonlinear spring is applied. The influence of essential parameters such as the nonlinear damping or stiffness on vibration, near the main parametric resonance region, are carried out numerically and next verified experimentally in a special experimental rig. Results show that the magnetorheological damper, together with the nonlinear spring can be efficiently used to change the dynamic behaviour of the system. Furthermore, the nonlinear elements applied in the suspension of the autoparametric system allow to reduce the unstable areas and chaotic or rotating motion of the pendulum.

1. Introduction

Dynamic mechanical systems possessing the pendulum arise in many practical application including special dynamical dampers [1]. The pendulum dynamics has been used for vibration suppression of a helicopter blade under flutter conditions [2]. Harmonically excited pendulum systems may undergo complicated dynamics, in particular if the pendulum and the oscillator are coupled by inertial resonance condition [3]. It has been found that the system generates various type of motion, from simple periodic oscillation to complex chaos. The presence of the coupling terms can lead to a certain type of instability which is referred as the autoparametric resonance. This kind of phenomenon takes place when the external resonance and the internal resonance meet due to the coupling terms. Small parametric excitations or small change of initial conditions may produce large response when the frequency of the excitations is close to one of the natural frequencies of the system.

A condition of the existence of an autoparametric vibrations is that, the structure has to consists at least of two constituting subsystems. The first one is a primary system that usually is excited by eternal force. The second subsystem, called as secondary, is coupled to the primary system by inertia terms. A classical example of an autoparametric system is the pendulum mounted to the oscillator, where the pendulum can both, oscillate or rotate [4]. Interesting example occurs when the primary system is at rest while the secondary system is vibrating. This phenomenon is called the dynamic vibration suppression.

In this paper we propose the concept of the use of combination of the magnetorheological damper together with the nonlinear spring applied in the autoparametric system suspension. Changing magnetorheological damping or nonlinear stiffness of the supporting spring, dangerous regions can be eliminated or moved away. This solution with MR damper gives reliable control possibilities and can help to react properly in critical situations. This kind of semiactive isolator can change dynamic behaviour to prevent undesired vibration or react properly according to varied initial conditions. The results are compared with a system with a classical viscous damper and a linear spring. The proposed idea can be used to design control strategy of an autoparametric system with an attached pendulum.

2. Model of a System with Semiactive Suspension

A model of the vibrating autoparametric system consists of a nonlinear oscillator (the primary system) with mass m_1 and the pendulum (the secondary system) made of two masses m_2 and m_p (Figure 1). Coordinate x represents the oscillator motion, and φ is an angle of the pendulum's rotation. The primary system is excited by classical linear spring with stiffness k_2 due to a harmonic motion of a base with frequency ω and amplitude Q. The stiffness of the oscillator's spring is assumed to be nonlinear Duffing's type and is described by parameters k and k_1. The length of the pendulum is denoted as l and its damping in journal bearings is assumed as linear and expressed by c_φ coefficient.

Determining the kinetic, potential energies, dissipation function of the system, and then applying Lagrange's equations of the second kind we receive governing equations of motion:

$$\begin{aligned}
&(m_1 + m_2 + m_p)\ddot{x} + c\dot{x} + d\tanh(e\dot{x}) + (k + k_2)x + k_1x^3 \\
&\quad + \left(m_2 + \frac{1}{2}m_p\right)l(\ddot{\varphi}\sin\varphi + \dot{\varphi}^2\cos\varphi) = k_2Q\cos\omega t, \\
&\left(m_2 + \frac{1}{3}m_p\right)l^2\ddot{\varphi} + c_\varphi\dot{\varphi} + \left(m_2 + \frac{1}{2}m_p\right)l(\ddot{x} + g)\sin\varphi = 0.
\end{aligned} \tag{2.1}$$

In nondimensional form, these equations can be written as

$$\begin{aligned}
&\ddot{X} + \alpha_1\dot{X} + \alpha_3\tanh(e\dot{X}) + X + \gamma X^3 + \mu\lambda\left(\ddot{\varphi}\sin\varphi + \dot{\varphi}^2\cos\varphi\right) = q\cos\vartheta\tau, \\
&\ddot{\varphi} + \alpha_2\dot{\varphi} + \lambda(\ddot{X} + 1)\sin\varphi = 0,
\end{aligned} \tag{2.2}$$

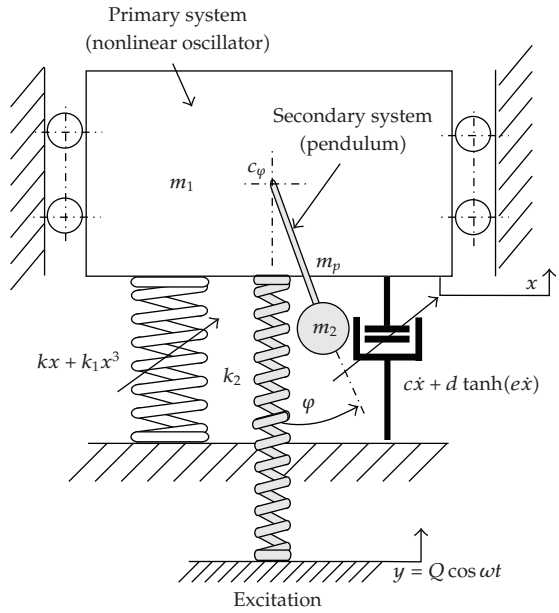

Figure 1: Model of an autoparametric system with a pendulum and semiactive suspension composed of MR damper and nonlinear spring.

where $X = x/x_{\mathrm{st}}, \varphi \equiv \varphi, \tau = \omega_0 t, \tau$ means dimensionless time, $\omega_0 = \sqrt{(k+k_2)/(m_1+m_2+m_p)}$ is the natural frequency of the oscillator together with a fixed pendulum, x_{st} is the static displacement of the linear oscillator. Definitions of dimensionless parameters are

$$\alpha_1 = \frac{c}{(m_1+m_2+m_p)\omega_0}, \qquad \alpha_2 = \frac{c_\varphi}{(m_2+(1/3)m_p)l^2\omega_0},$$
$$\alpha_3 = \frac{d}{(m_1+m_2+m_p)\omega_0^2 x_{\mathrm{st}}}, \qquad \gamma = \frac{k_1}{k+k_2}x_{\mathrm{st}}^2, \qquad \lambda = \frac{(m_2+(1/2)m_p)x_{\mathrm{st}}}{(m_2+(1/3)m_p)l}, \tag{2.3}$$
$$\mu = \frac{(m_2+(1/3)m_p)l^2}{(m_1+m_2+m_p)x_{\mathrm{st}}^2}, \qquad q = \frac{k_2 Q}{(k+k_2)x_{\mathrm{st}}}, \qquad \vartheta = \frac{\omega}{\omega_0},$$

where $x_{\mathrm{st}} = (m_1+m_2+m_p)g/(k+k_2)$.

Damping of the oscillator is studied in two variants, as linear viscous and nonlinear magnetorheological. Our concept of nonlinear damping is realized by application of the magnetorheological (MR) damper. The first step is to describe the nonlinear behaviour of the MR damper and to propose a proper mathematical model which characterizes its real behaviour. The characteristics are found by taking the sampled restoring force and input velocity based on the experimental data and curve fittings of a real MR damper. We propose to use a smooth function of modified Bingham's model suggested in paper [5]

$$F_d = d\tanh(e\dot{x}) + c\dot{x}, \tag{2.4}$$

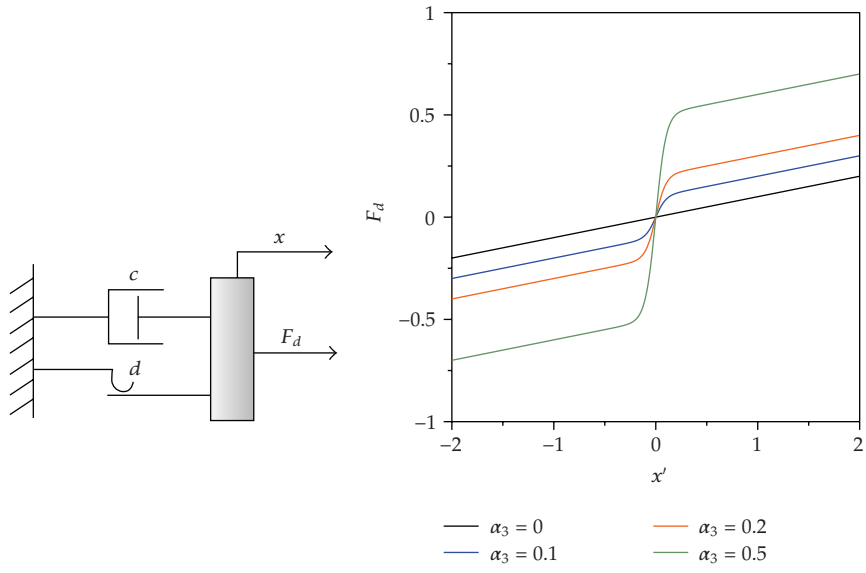

Figure 2: The Bingham model of MR damper (a) and exemplary characteristics for varied α_3 and $\alpha_1 = 0.1$ for $e = 10$ (b).

where d is the force coefficient related to the rheological behaviour, produced by the fluid, $\dot{x}$ is the piston velocity of MR damper. In (2.4) e is a constant. In our study we assumed this value is equal to ten. In dimensionless form of this equation is expressed as

$$F_d = \alpha_3 \tanh\left(e\dot{X}\right) + \alpha_1 \dot{X}, \tag{2.5}$$

where α_3 is dimensionless coefficient of MR damping defined as

$$\alpha_3 = \frac{d}{\left(m_1 + m_2 + m_p\right)\omega_0^2 x_{\mathrm{st}}}. \tag{2.6}$$

Equation (2.6) presents the restoring force of the MR damper with respect to the input velocity and acceleration.

The considered MR model consists of a combination of viscous damping (α_1) and a Coulomb's friction (α_3), as shown in Figure 2(b). The Bingham's rheological model can be used successfully when the width of hysteretic loop in real characteristics of MR dampers is relatively narrow [6]. However, if the hysteretic loop is wider, it is necessary to construct a more complicated rheological model.

Analytical solutions near the main parametric resonance received by the harmonic balance method for the system with typical linear viscous damping are presented in paper [1].

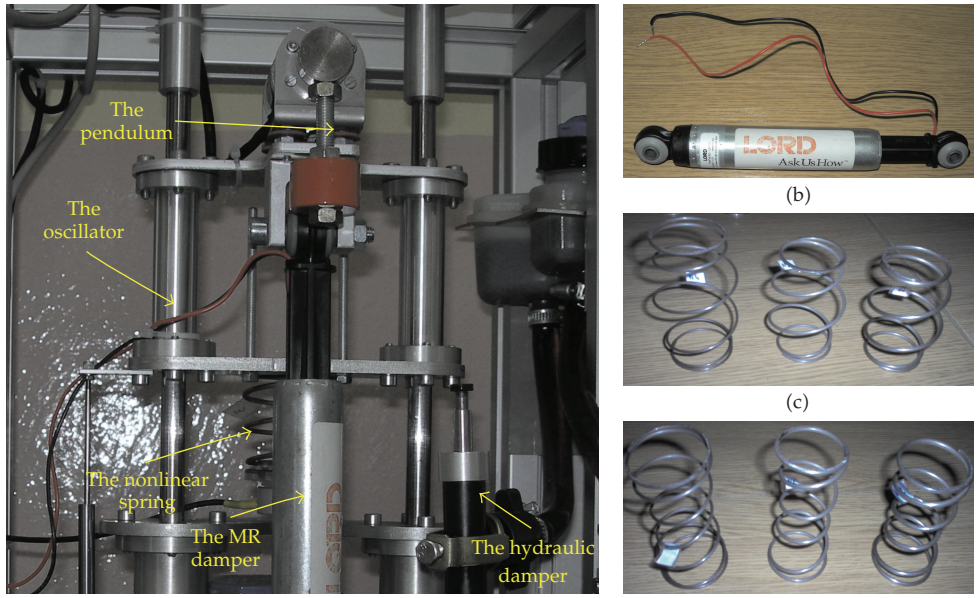

Figure 3: Photo of experimental rig (a), magnetorheological damper RD 1097-01 (b), and nonlinear oscillator springs (c, d).

3. Experimental Setup

The experiment was performed on an autoparametrically two degree of freedom system presented in Figure 3 and schematically in Figure 1. Figure 3(a) shows a photo of the main parts of a mechanical system while nonlinear components of suspension, that is, MR damper *RD 1097-01* and nonlinear spring are presented in Figures 3(b), 3(c), and 3(d). Detailed description of the laboratory rig can be found in paper [7]. The spring which connects the oscillator and the base is considered in two variants, linear or nonlinear with different soft or hard stiffness characteristics. Nonlinearity of springs have been reached by designing of a special shape of springs: barrel shape (Figure 3(c)) and spiral hourglass helical shape (Figure 3(d)).

A semiactive control system typically requires a small external power source for operation. Moreover, the motion of the structure can be used to develop the control forces. Therefore, semiactive control systems do not have the potential to destabilize the structural system, in contrast to active systems. Many studies have indicated that semiactive systems perform significantly better than passive devices [8–10]. A smart isolation system for the base isolated, two-degree-of-freedom structural model employing MR dampers was investigated experimentally by Yoshioka et al. [11].

In our experimental system we use magnetorheological damper *RD 1097-01* produced by *Lord Corporation* [12]. In earlier studies we used a typical hydraulic damper with an oil tank. Contrary to the hydraulic damper, MR damper does not require mechanical valves to control flow. Magnetorheological fluids (MRF) are a class of materials whose rheological properties are rapidly varied by applying a magnetic field. This change is in proportion to the magnetic field applied and is immediately reversible. Voltage in the electromagnet coils creates a magnetic field around the fluid gap between the housing and the piston. When it is

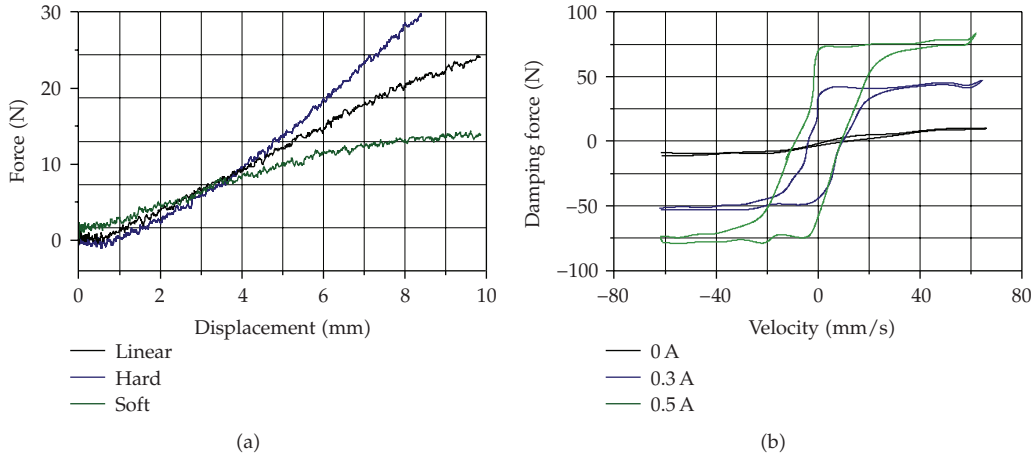

Figure 4: Exemplary characteristics of different springs (a) and nonlinear damping force of MR versus velocity of the damper piston (b).

not activated, MR fluid behaves like a free flowing liquid, with a consistency similar to that of typical oil. Furthermore, this kind of smart materials provides simple, quiet and rapid response between the electronic control and mechanical system. The magnetorheological materials are useful in many applications because the change in their material properties is large.

The magnetorheological damper *RD 1097-01* is suitable for light structure suspensions and isolation applications. The functional parameters of the damper listed by the manufacturer take values: maximum force 100 N (for current 1 A and piston velocity 51 mm/s), stroke ±25 mm, response time 25 ms. The force in the passive-off-mode (0 A) is about 9 N.

Such parameters allow very low damping force if the damper has to be switched off. In Figure 4(b) experimental characteristics of MR damper *RD 1097-01*, for different current intensity are shown. In Figure 4(a) exemplary characteristics of nonlinear springs used in experimental system are presented. The spring corresponding to linear characteristic is denoted as no. 1, hard characteristic as no. 2 ($k = 10^3\,\mathrm{N/m}$, $k_1 = 5 \cdot 10^6\,\mathrm{N/m^3}$) and soft characteristic as no. 3 ($k = 2.5 \cdot 10^3\,\mathrm{N/m}$, $k_1 = -9 \cdot 10^6\,\mathrm{N/m^3}$). Six different types of linear and six nonlinear springs are used in the equipment.

4. Dynamics of MR Damped System

In this type of the systems near the parametric resonances the unstable areas may occur, and moreover, for certain parameters chaotic motion may be observed [13]. Due to strong nonlinearities, the global and local dynamics of the system is studied by direct numerical simulations of (2.2). The equations have been implemented in Matlab-Simulink and Dynamics packages [14]. The software allows to consider bifurcation diagrams, Poincaré maps, phase trajectories, time histories, basins of attraction and two parameter plots. Because the damping force F_d, generated by MR damper, is approximated by a smooth function (2.5), the fourth-order Runge-Kutta method is used for numerical integration. The simulations are carried out on the basis of data taken from the laboratory rig. In these simulations

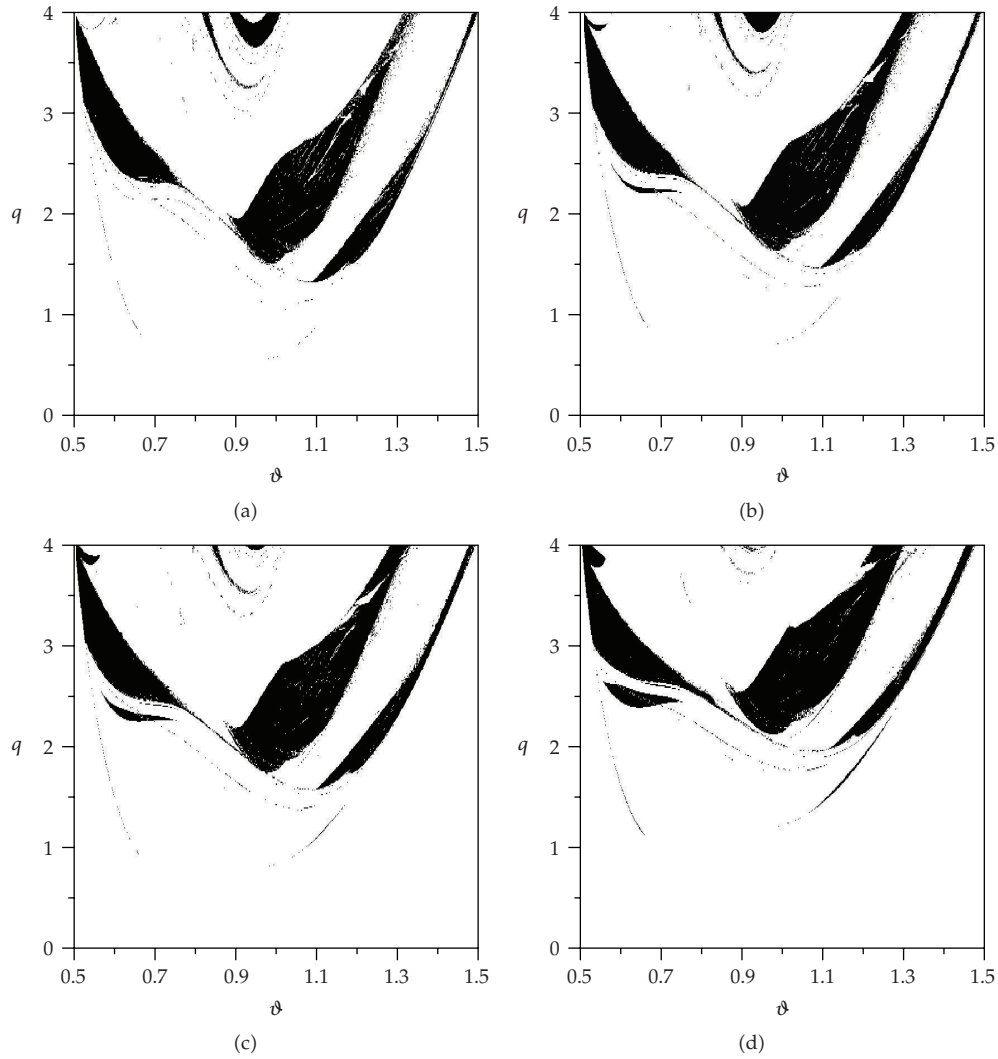

Figure 5: Two parameter space plot for different settings of MR damping $\alpha_3 = 0$ (a), $\alpha_3 = 0.1$ (b), $\alpha_3 = 0.2$ (c) and $\alpha_3 = 0.5$ (d) for $\gamma = 0$.

the following parameters are used: $\alpha_1 = 0.26$, $\alpha_2 = 0.1$, $q = 3$, $\mu = 17.2$, and $\lambda = 0.12$. The first 500 excitation periods were excluded in the analysis presented in this section.

The bifurcation diagrams are calculated to investigate the effects of the influence of MR damping on dynamics for typical resonance range. For each value of the varied parameter, the same initial conditions are used so that the comparison could be made between different system's parameter values.

Figure 5 depicts two parameter space plots with a set of initial conditions $\varphi_o = 0.1$, $\varphi'_o = 0$, $x_o = 0$, $x'_o = 0$. The black colour regions indicate chaotic motions estimated on the basis of positive value of all Lyapunov exponents. Unmarked areas (white colour) define periodic motion (oscillation or rotation) or regions where pendulum is at rest. The main parametric resonance appears near the frequency ratio $\vartheta \approx 1$.

We propose to change the dynamic behaviour of the autoparametric system (for example transfer chaotic motion into periodic) by using MR damper which could allow for a change of the system motion online. The MR damper is a semiactive device, this means that the damping force can only be commanded by the input voltage adjusted to the MR damper. Therefore, the dynamic mechanism of the system with installed MR damper in the suspension can be updated in an online adaptive manner, according to the required conditions. In spite of the fact MR damper cannot activate positive force, the advantage is that the restoring force can be modified online without stopping the system.

Introducing MR damping we observe, that chaotic resonance tongues move towards the axis of amplitude of excitation q. Additionally, small chaotic zones (black colours) are reduced and a part of the chaotic area is divided into smaller regions (Figure 5).

To have better insight into the parameters space plot, the bifurcation diagrams (crosschecks) have been done. Figures 6(a) and 6(b) present the numerical bifurcation diagram and Lyapunov exponent corresponding to the classical viscous damped model ($\alpha_3 = 0$). The positive value of the maximal Lyapunov exponent indicates that the black area in bifurcation diagrams represents the chaotic regions. For the frequency of $\vartheta \approx (0.65–1.16)$ pendulum goes to rotation. This result has been obtained by experimental results. Surprisingly, the activated MR damping causes an increase in the second chaotic area (near $\vartheta \approx 1.2$) (Figures 6(c) and 6(d)) reducing rotation of the pendulum. The first chaotic zone ($\vartheta \approx 0.54–0.62$) remains practically unchanged.

The rotation of pendulum is defined as a case when the motion amplitude exceeds $\varphi = \pm\pi$ [15].

Interesting example is observed for frequency $\vartheta \approx 1.3$. The pendulum goes from lower to the upper position and is stopped there. The inverted pendulum's equilibrium point becomes stable. The same result is obtained from experimental tests (the grey line in Figure 7(a)). But, for frequency $\vartheta \approx 1.4$ (Figure 7(b)) the pendulum executes the "*chaotic swinging*" in lower position with positive value of Lyapunov exponent (Figure 6(b)). This result has not been confirmed on the experimental rig. This chaotic region is very narrow and therefore probably because of dynamically changed damping of the pendulum's pivot and varying working conditions, this result is difficult to find by the experiment. This may also be caused by the system sensitivity to the initial conditions.

Introduction of MR damping does not change stability of the inverted pendulum for analyzed range of parameter α_3. However, further increase of MR damping above the certain critical value change the inverted pendulum from stable into unstable.

5. Suspension with a Nonlinear Spring

Another proposal to change the system dynamics is modification of nonlinear stiffness of a spring mounted in the suspension. Warminski and Kecik [1] proved that introduction of nonlinear stiffness seems to be a promising method for improving the phenomenon of dynamical vibration absorption, but for some parameters this solution can produce new, unwanted attractors. Comparison of the parameter space plots for the system with the linear spring (Figure 5(a)) and the nonlinear springs Figures 8(a) and 8(b), shows that for stiff characteristics the chaotic resonance tongues are moved to the right side. Furthermore, the small resonance area (black colour), near $\vartheta \approx 0.9$ and $q \approx 4$, disappears.

The bifurcation diagrams for varying ϑ for the hard nonlinear spring are shown in Figure 9. The stiffness causes mainly an increase of the second chaotic area (left-side)

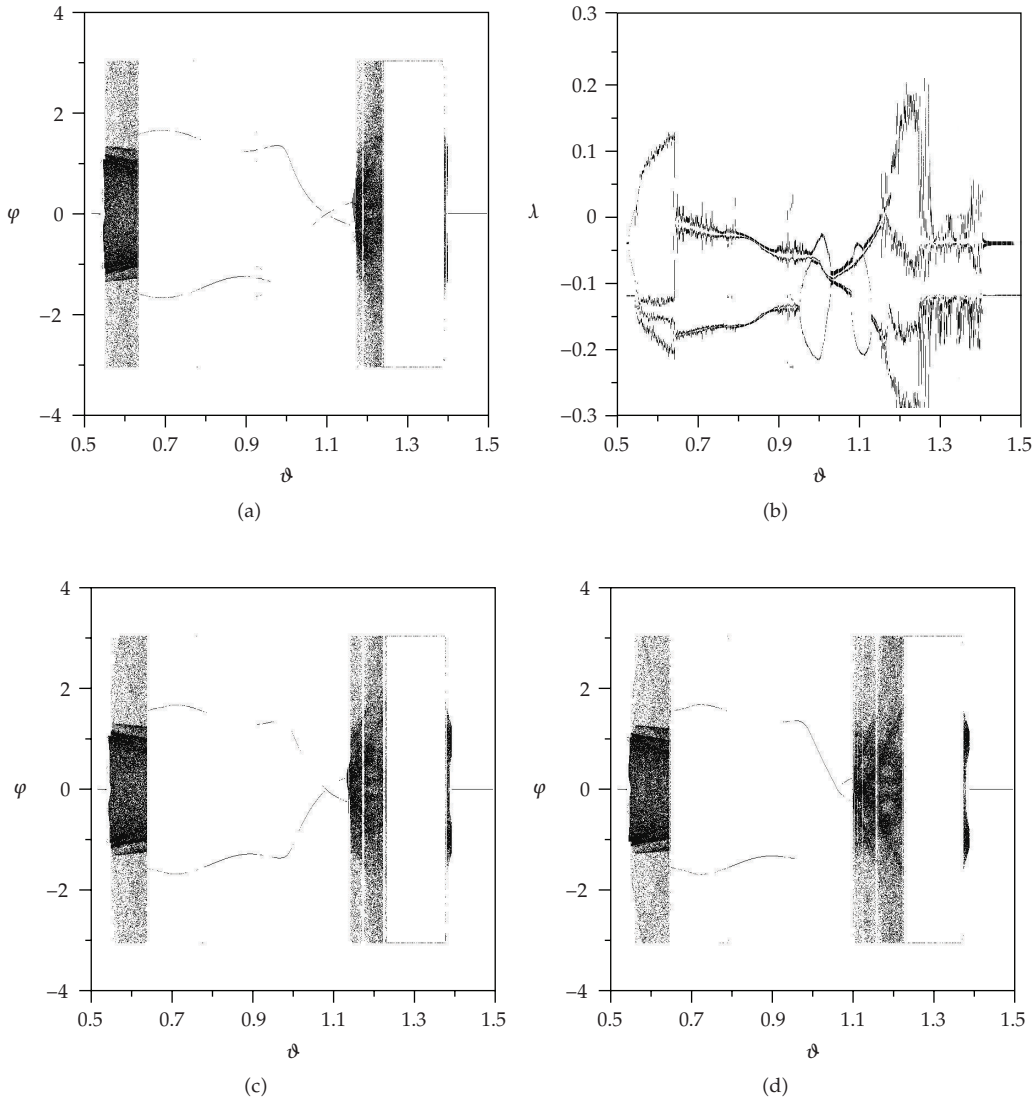

Figure 6: Bifurcation diagrams φ versus ϑ obtained for $\alpha_3 = 0$ (a), $\alpha_3 = 0.1$ (c), $\alpha_3 = 0.2$ (d), and Lyapunov exponents obtained for $\alpha_3 = 0$ (b), calculated for a system with a linear spring.

and additionally, for nonlinearity $\gamma = 0.02$ (Figure 9(b)), the stabilisation of the inverted pendulum is eliminated. The first chaotic zone is shifted towards to the second chaotic region. This effect can be explained by stiffening effect of the suspension. Obtained results show that hard stiffness of a spring can be used for avoidance unwanted dynamical situations.

Figure 10 demonstrates the influence of soft nonlinearity of a spring on the main parametric resonance. The soft nonlinearity slightly moves the resonance tongue to left-side. Additionally, near the frequency $\vartheta \approx 0.8$, for $\gamma = -0.002$ new bifurcation points exist. Therefore, it is very important to check the existence a new attractors if spring with soft characteristic is to be applied.

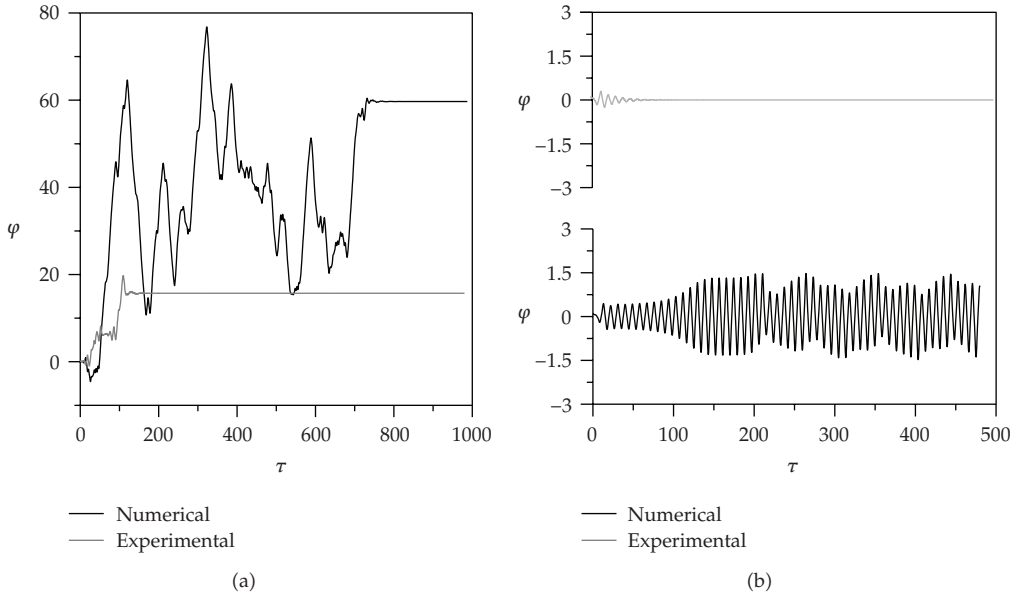

Figure 7: Time history of pendulum motion for frequency $\vartheta = 1.3$ (a) and $\vartheta = 1.4$ (b) for $\gamma = 0$ and $\alpha_3 = 0$.

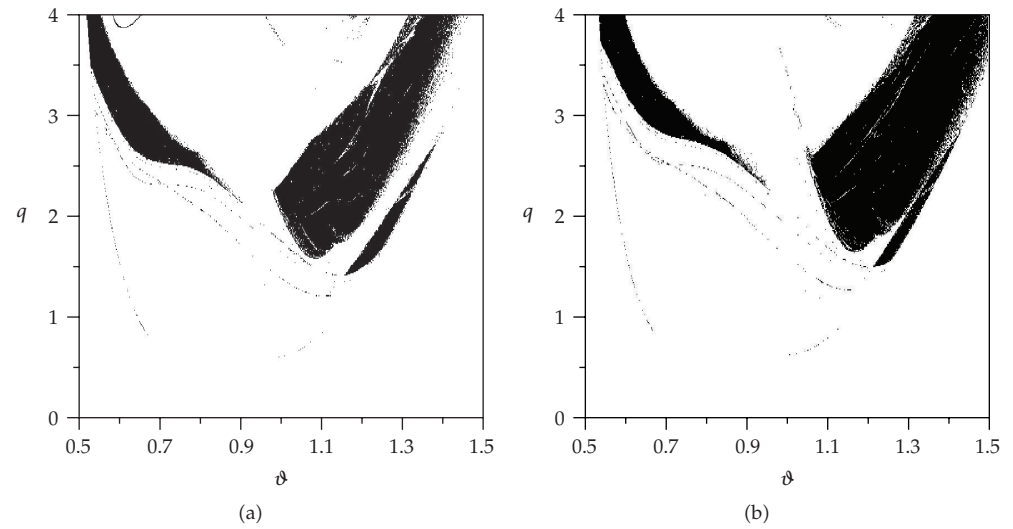

Figure 8: Parameter space plot of a pendulum for different values of hard stiffness $\alpha_3 = 0$, $\gamma = 0.01$ (a) and $\gamma = 0.02$ (b) for $\alpha_3 = 0$.

6. Dynamics Control of a System with Semi-Active MR Suspension

In real dynamical autoparametric structure, it is very important to keep the pendulum at a given, wanted attractor. The nonlinear systems are sensitive for initial conditions, environmental or working conditions, therefore monitoring of suitable parameters is required to improve dynamic. The existence of two or more solutions for the same parameter values in a nonlinear system indicates that the initial conditions play a critical role in determining

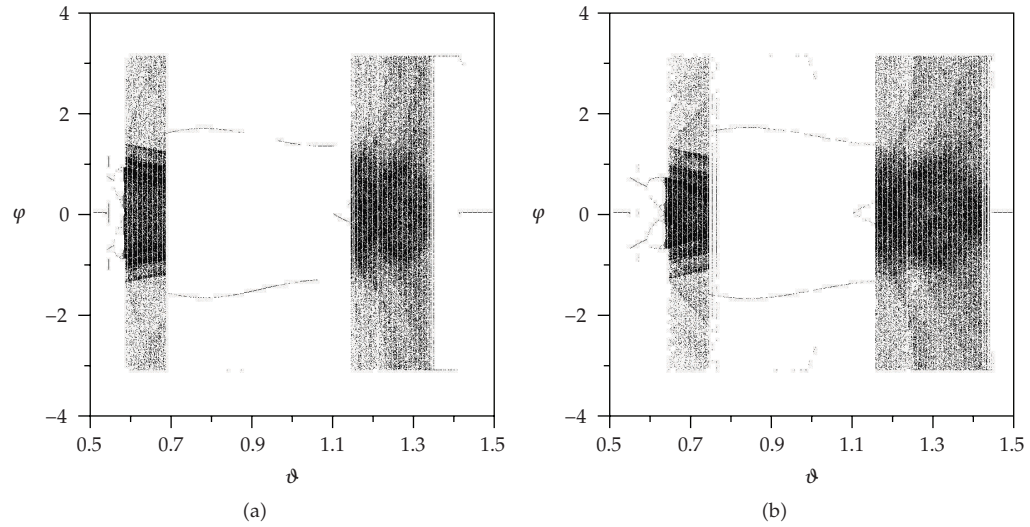

Figure 9: Bifurcation diagrams φ versus ϑ obtained for $\gamma = 0.01$ (a), $\gamma = 0.02$ (b) and $\alpha_3 = 0$.

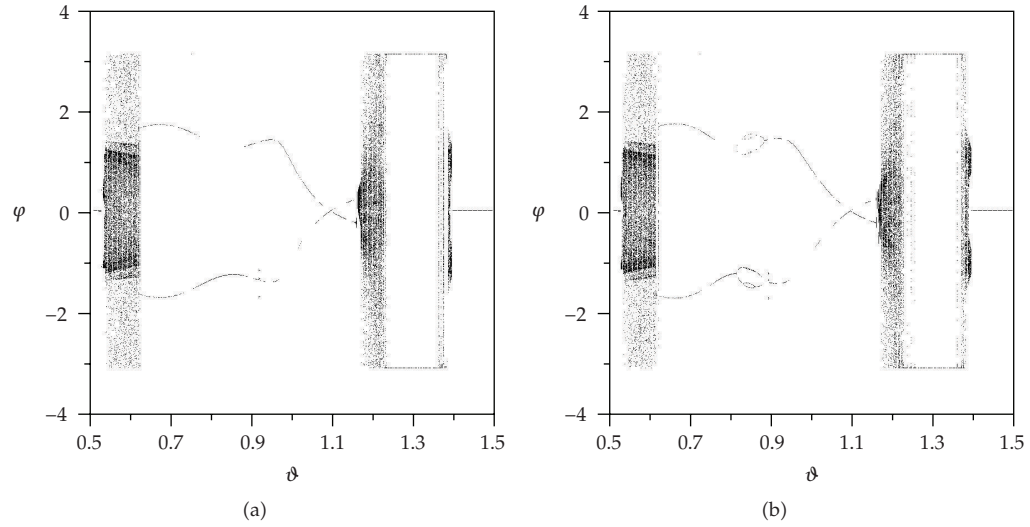

Figure 10: Bifurcation diagrams φ versus ϑ obtained for $\gamma = -0.001$ (a) $\gamma = -0.002$ (b) and $\alpha_3 = 0$.

the system's overall response. Therefore, slight disturbance may cause a jump from the oscillating pendulum to the rotation or chaotic motion.

Figure 11(a) shows basins of attractions for two sets of initial conditions of the pendulum, that is, its angular displacement and angular velocity. The plot (Figure 11) indicates more than one coexisting attractor for the same set of parameters. For each attractor, the set of initial conditions leading to long-time behaviour is plotted in corresponding colours. We observe two double-point attractors and one one-point attractor with the suitable basin of attraction. Attractor no. 1, with basins of attraction in a dark grey colour, represents example of a semitrivial solution where the pendulum does not move while the oscillator

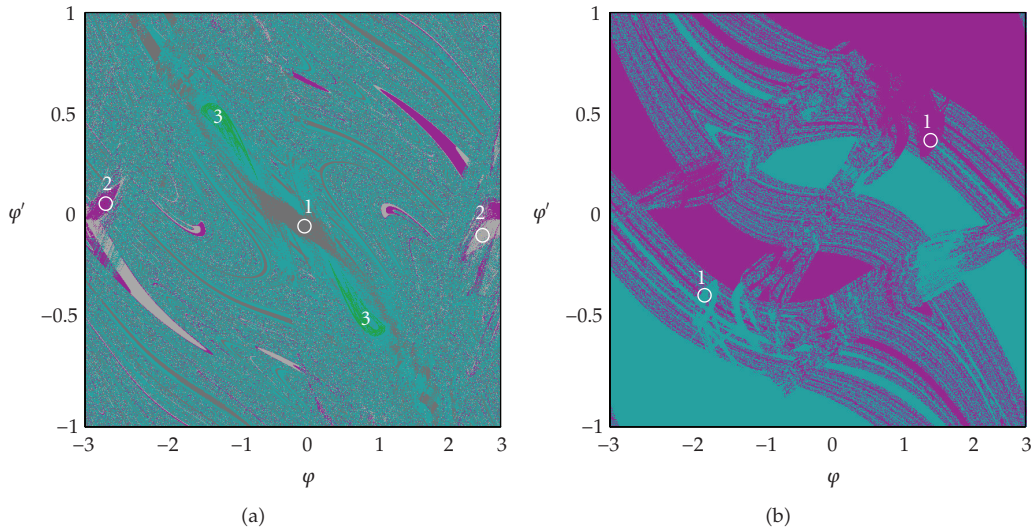

Figure 11: Basins of attraction of a pendulum for $\vartheta = 1.4$ (a) and $\vartheta = 0.7$ (b) obtained for $\alpha_3 = 0$, $\gamma = 0$.

vibrates having the pendulum as an additional mass. Attractor no. 2 represents swinging of the pendulum in the upper position (around the point $\varphi \approx \pi$). Its basins of attraction, denoted as light grey, show swinging with a shift on the right side ($\varphi \approx \pi - \delta$), a pink colour corresponds to relevant swinging of the pendulum with a left-side shift ($\varphi \approx \pi + \delta$), where δ is a shift of vibration centre of the pendulum in the upper position. The two possible shifts are symmetric around the static position of the pendulum and depend on its initial conditions. The chaotic attractor and its basin of attraction are marked as green and light blue respectively. This attractor is responsible for "*chaotic swinging*" of the pendulum in lower position.

Time history of pendulum motion, for the case of chaotic swinging (attractor no. 3) obtained from numerical simulation is plotted in Figure 12(a). However, if the MR damping is activated during the motion, for short instance of time of about value $\alpha_3 = 0.25$, then the trajectory "jumps" from attractor no. 3 into no. 1. The same result is obtained by experimental test (Figure 12(b)). It confirms that MR damper applied in the suspension can be useful device to move pendulum's motion from unwanted, often dangerous situations. Swinging of the pendulum in inverted position (attractor no. 2) is presented in Figure 13(a). Nevertheless, if the MR damper is activated for a certain interval time then for $\alpha_3 = 0.11$ attractor no. 2 goes into attractor no. 3 representing chaotic swinging—a grey line, or for $\alpha_3 = 0.1$ goes into attractor no. 1 lower equilibrium position of the pendulum black line in Figure 13(b).

Figure 11(b) shows basins of attraction for frequency $\vartheta = 0.7$. In this case we observe one double-point attractor which represents rotation of the pendulum. The pink colour denotes positive rotation of the pendulum, the light blue colour is responsible for its negative rotation (clock wise). If the pendulum is to play a role of dynamical absorber, this kind of motion is usually unwanted. For certain parameters, the switch-on of the MR damping lead to transition a rotation to swinging of a pendulum or also can be used to a change of rotation direction. In order to obtain these results, time of MR damper being active must be longer and α_3 parameter should be of higher value.

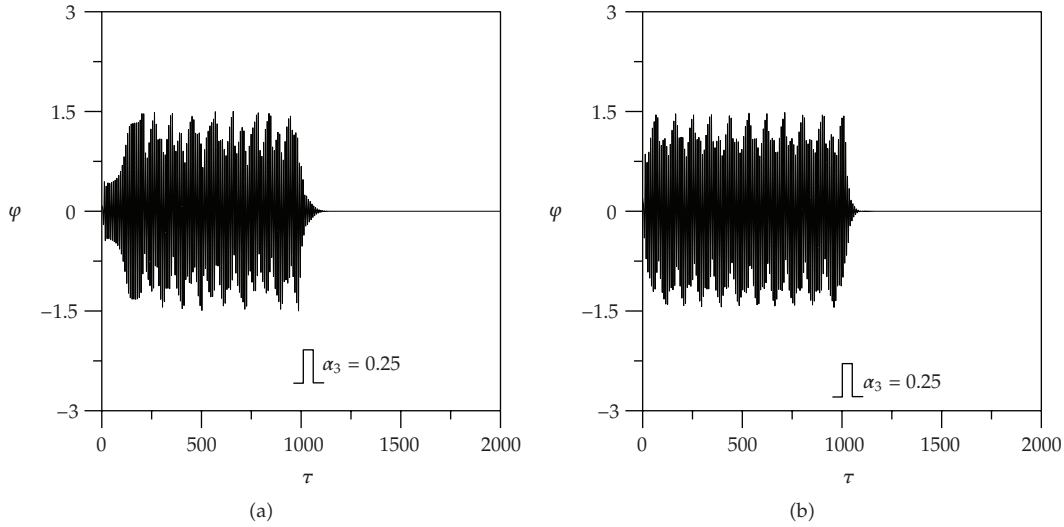

Figure 12: Time histories of a pendulum for $\vartheta = 1.4$, $\varphi_o = 0.1$: numerical (a) and experimental (b) results with impulse turn on of MR damping.

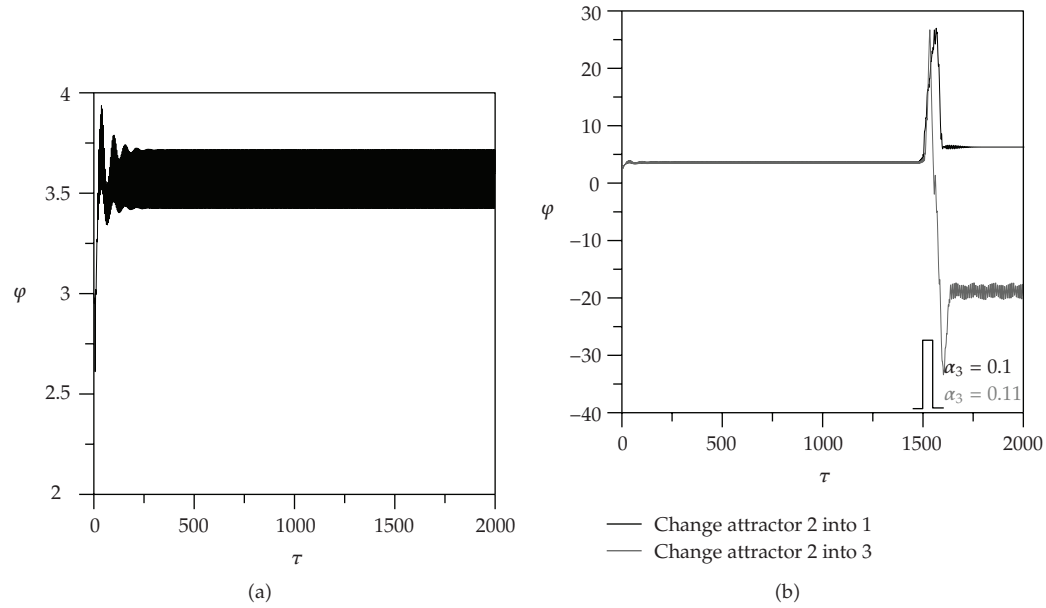

Figure 13: Time histories of a pendulum for $\vartheta = 1.4$, $\varphi_o = 3$ without MR damping (a) and with impulse turn on of MR damping (b).

In Figure 14(a) a coefficient of MR damping is equal $\alpha_3 = 1.1$ and its activation lasts $\tau \approx 500$. This causes the pendulum rotation to change from positive to negative. Magnetorheological damping can be applied also to stop the rotation of the pendulum.

Therefore, after proper tuning of the system the response can be modified from chaotic to periodic motion and vice versa. It has been confirmed experimentally that the simple open loop technique, allows for an easy control of the system response.

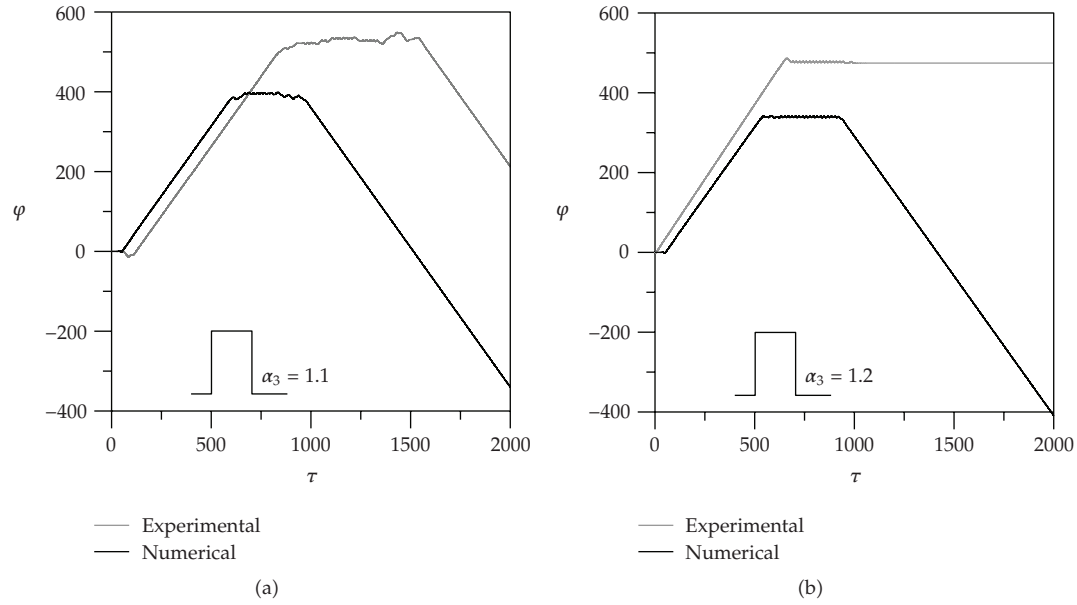

Figure 14: Numerical and experimental time histories of a pendulum motion for $\vartheta = 0.7$, $\varphi_o = 0.1$, $\alpha_3 = 1.1$ (a) and $\alpha_3 = 1.2$ (b), obtained for the system with a linear spring, $\gamma = 0$.

7. Conclusions and Final Remarks

This paper focuses on numerical and experimental investigations of an autoparametric system with a pendulum subjected to kinematic excitation. The dynamic response has been examined by constructing parameter plots which determinate the regular or irregular motion. The bifurcation diagram, Lyapunov exponents, time histories, and basins of attractions have been used to check nature of motion in those regions.

The results presented in the paper show that MR damping together with nonlinear spring included in the pendulum-like absorber structure can be an effective tool for reduction of dangerous unstable regions without a loss of the dynamical absorption effect. After proper tuning, the system can be maintained on a regular or a chaotic attractor. Moreover, by applying simple open loop control, it is possible to fit the structure response to the frequency of external excitation. Obtained results show that our semiactive suspension of the autoparametric system allows to freely move, both up and down, or left and right, the chaotic regions. Application of a closed loop control technique, leading to a smart dynamic absorber is a next step of our investigations.

References

[1] J. Warminski and K. Kecik, "Instabilities in the main parametric resonance area of a mechanical system with a pendulum," *Journal of Sound and Vibration*, vol. 322, no. 3, pp. 612–628, 2009.

[2] I. Nagasaka, Y. Ishida, T. Ishii, T. Okada, and T. Koyama, "Vibration suppression of helicopter blades by pendulum absorbers (analytical and experimental investigation in case of rigid-body mode)," *Transactions of the Japan Society of Mechanical Engineers Part C*, vol. 73, no. 725, pp. 129–137, 2007.

[3] J. Warminski and K. Kecik, "Autoparametric vibrations of a nonlinear system with pendulum," *Mathematical Problems in Engineering*, vol. 2006, Article ID 80705, 19 pages, 2006.

[4] K. Kecik and J. Warminski, "Magnetorheological damping of an autoparametrically excited system," in *Proceedings of the Euromech Conference*, vol. 498, pp. 186–192, 2008.
[5] D. Tang, H. P. Gavin, and E. H. Dowell, "Study of airfoil gust response alleviation using an electromagnetic dry friction damper—part 1: theory," *Journal of Sound and Vibration*, vol. 269, no. 3–5, pp. 853–874, 2004.
[6] G. M. Kamath, M. K. Hurt, and N. M. Wereley, "Analysis and testing of Bingham plastic behavior in semi-active electrorheological fluid dampers," *Smart Materials and Structures*, vol. 5, no. 5, pp. 576–590, 1996.
[7] J. Warminski and K. Kecik, "Regular and chaotic motions of an autoparametric real pendulum system with the use of a MR damper," *Modelling, Simulation and Control of Nonlinear Engineering Dynamical Systems*, pp. 267–276, 2009.
[8] G. W. Housner, L. A. Bergman, T. K. Caughey et al., "Structural control: past, present, and future," *Journal of Engineering Mechanics*, vol. 123, no. 9, pp. 897–971, 1997.
[9] T. T. Soong and B. F. Spencer, "Supplemental energy dissipation: state-of-the-art and state-of-the-practice," *Engineering Structures*, vol. 24, no. 3, pp. 243–259, 2002.
[10] M. D. Symans and M. C. Constantinou, "Semi-active control systems for seismic protection of structures: a state-of-the-art review," *Engineering Structures*, vol. 21, no. 6, pp. 469–487, 1999.
[11] H. Yoshioka, J. C. Ramallo, and B. F. Spencer, ""Smart" base isolation strategies employing magnetorheological dampers," *Journal of Engineering Mechanics*, vol. 128, no. 5, pp. 540–551, 2002.
[12] http://www.lord.com/.
[13] K. Kecik and J. Warminski, "Analysis of chaotic and regular motions of an autoparametric system by recurrence plots applications," *Vibrations in Physical Systems*, vol. 2, pp. 221–226, 2010.
[14] H. E. Nusse and J. A. Yorke, *Dynamics: Numerical Explorations*, vol. 101 of *Applied Mathematical Sciences*, Springer, New York, NY, USA, 1994.
[15] M. J. Clifford and S. R. Bishop, "Rotating periodic orbits of the parametrically excited pendulum," *Physics Letters A*, vol. 201, no. 2-3, pp. 191–196, 1995.